Explorations of Magnetic Properties of Noble Gases: The Past, Present, and Future

Włodzimierz Makulski

Faculty of Chemistry, University of Warsaw, 02-093 Warsaw, Poland; wmakul@chem.uw.edu.pl;
Tel.: +48-22-55-26-346

check for
updates

Abstract: In recent years, we have seen spectacular growth in the experimental and theoretical investigations of magnetic properties of small subatomic particles: electrons, positrons, muons, and neutrinos. However, conventional methods for establishing these properties for atomic nuclei are also in progress, due to new, more sophisticated theoretical achievements and experimental results performed using modern spectroscopic devices. In this review, a brief outline of the history of experiments with nuclear magnetic moments in magnetic fields of noble gases is provided. In particular, nuclear magnetic resonance (NMR) and atomic beam magnetic resonance (ABMR) measurements are included in this text. Various aspects of NMR methodology performed in the gas phase are discussed in detail. The basic achievements of this research are reviewed, and the main features of the methods for the noble gas isotopes: ^{3}He, ^{21}Ne, ^{83}Kr, ^{129}Xe, and ^{131}Xe are clarified. A comprehensive description of short lived isotopes of argon (Ar) and radon (Rn) measurements is included. Remarks on the theoretical calculations and future experimental intentions of nuclear magnetic moments of noble gases are also provided.

Keywords: nuclear magnetic dipole moment; magnetic shielding constants; noble gases; NMR spectroscopy

1. Introduction

The seven chemical elements known as noble (or rare gases) belong to the VIIIa (or 18th) group of the periodic table. These are: helium ($_2$He), neon ($_{10}$Ne), argon ($_{18}$Ar), krypton ($_{36}$Kr), xenon ($_{54}$Xe), radon ($_{86}$Rn), and oganesson ($_{118}$Og). Their positions in the periodic table of elements are still the subject of some controversy [1]. Noble gases at normal conditions are colorless, odorless, and nonflammable monoatomic gases. The completed valence electron in the outer shell leads to this species having very low chemical activity, and they are then termed as inert gases [2]. However, several covalent and additive species of xenon are known today, mainly with strongly reducing fluorine and oxygen atoms [3]. Noble gases can be found in the Earth's atmosphere in trace amounts: 0.00052% of helium, 0.0018% of neon, 0.93% of argon, 0.00011% of krypton, 0.0000087% of xenon, and 6×10^{-18} molar percent of radon.

Certain isotopes of noble gases possess intrinsic magnetic properties, such as a nuclear spin number (I) and as their nuclear magnetic moments (NMMs). There is no reason to doubt the importance of these parameters for the broad field of chemical and physical phenomena. The aim of this review is to show the developments of nuclear magnetic resonance (NMR) spectroscopy in the field of precisely establishing nuclear dipole moments for nuclei that belong to the group of noble gases. Experiments involving gas phase NMR achievements [4,5] are discussed in detail along with the new developments of different methods leading to measurements and theoretical calculations of the magnetic properties of noble gases.

It is clear that nuclear magnetic moments, along with the shape and size of nuclei and quadrupole moments, play an important role in discussions regarding the structure and behavior of nuclear composition. The spectacular growth of theoretical studies using different methods [6] needs more precise experimental values for the comparison and verification of results. Since the early measurements in atom-molecular beam experiments performed by I.I. Rabi et al. [7] between 1930 and 1937, NMR has played a crucial role in establishing the first magnetic moments of nuclei. Particularly, more accurate NMR results can be received when gas phase experiments are performed. The radiofrequency spectra for isolated atoms or molecules can be relatively easily measured when new, advanced NMR spectrometers are used. The calculations of diamagnetic effects, also known as shielding effects present in any atom or molecule, are crucial for precise calculations. In this case, high-level theoretical computations can be performed for a single atom at room conditions. If we join both these kinds of examinations, a full analysis of nuclear moments is possible [4,5].

It is well known that noble gas atoms have very long nuclear spin relaxation times [8]. This leads to very narrow NMR resonance lines and high digitalization of the spectra is possible. Very narrow lines are noticed even for quadrupolar nuclei due to the spherical symmetry of the electron distribution in atoms. The effect of the surface-to-volume ratio and temperature can change the relaxation times only to an extent. It is very useful that gaseous signals for different density samples can be measured with good precision.

2. Investigation of Nuclear Magnetic Moments (NMMs) by Experiment and Theory

2.1. Definition of Nuclear Magnetic Moment

The nuclear system is a complex physical structure consisting of nucleons, i.e., protons and neutrons [9]. The nuclei in atoms or molecules have several physical properties that define their behavior. These are the mass, electric charge, shape and radius, and electromagnetic moments and spin. The magnetic moment of nucleus X is expressed in the following form [10]:

$$\mu_X = g_X \times \mu_N \times I_X \tag{1}$$

where I_X is the so-called spin, g_X is the g nuclear factor of nucleus X, and the constant $\mu_N = e\hbar/2m_p$ (where m_p is the proton mass) is known as the nuclear magneton $\mu_N = 5.05078353(13) \times 10^{-27}$ J/T [11]. In an external magnetic field oriented along the axis z, a magnetic vector of nucleus with spin I may receive $2I + 1$ orientations with $I_Z = m_I\hbar$, which are characterized by the magnetic quantum numbers m_I, where $-I \leq m_I \leq I$.

In experiments performed in uniform magnetic fields, only one component of the NMM can be observed in direction z of the applied field. This is often called the nuclear magnetic moment value itself. As the NMM is a vector, the full magnitude is $\mu_X(\sqrt{I_X(I_X+1)}/I_X$. The magnetic properties of a given nuclei can also be emphasised as the gyromagnetic ratio (magnetogyric ratio) γ_X. γ_X is the ratio of its magnetic moment to its angular momentum: $\gamma_X = g_X \times \mu_X/\hbar$ in rad s^{-1}T^{-1} units. When divided by the 2π factor, the gyromagnetic ratio is often used in NMR spectroscopy because of its direct proportionality to the resonance frequency of the nucleus under consideration. Several compilations of NMR frequencies in different magnetic fields expressed in induction units (B_0) are well known (see e.g., Bruker Almanach).

A few theoretical models can predict the value of the magnetic dipole moment, and there are several experimental techniques aimed at carrying out measurements in nuclei within the nuclear chart. They will be presented for noble gas nuclei in the next sections of this paper.

2.2. Nuclear Magnetic Resonance (NMR) Procedure for Accurate NMM Determination

NMR spectroscopy belongs to the methods that are often used for precisely measuring the nuclear magnetic moments of different stable nuclei [12]. As NMR spectroscopy relies on the photon absorption

of quantum energy that corresponds to the radio frequency region, the transition between the two states can be formulated as:

$$\Delta E = h \times \Delta \nu \tag{2}$$

where h is Planck's constant (h = $6.62607004 \times 10^{-34}$ J s). In NMR and Magnetic resonance imaging (MRI), the quantity $\Delta \nu$ is called the resonance or the Larmor frequency. When the energy of the photon matches the energy difference between the two spin states, an absorption of energy occurs. The resonance frequency ν_X for nucleus X in the isotropic medium is proportional to the external magnetic field induction B_z [10]:

$$h\nu_X = \Delta\mu_X^z (1 - \sigma_X)B_z \tag{3}$$

where $\Delta\mu_X^z$ is the transition-related change of the projection of the magnetic moment on the z field axis, and σ_X is the shielding parameter. An analogous equation can be written for the other nuclei placed in the same magnetic field:

$$h\nu_Y = \Delta\mu_Y^z (1 - \sigma_Y)B_z \tag{4}$$

A precise solution of Equations (3) and (4) is difficult as the measuring of magnetic fields is usually a complicated task. Thus, it is convenient to divide both equations by pages, eliminating the external magnetic field induction B_z, and to use the final formula crucial for establishing the NMM using NMR spectroscopy [4,5]:

$$\Delta\mu_X^z = \frac{\nu_X}{\nu_Y} \times \frac{(1 - \sigma_Y)}{(1 - \sigma_X)} \times \frac{I_X}{I_Y}\Delta\mu_Y^z \tag{5}$$

This relationship is a rule for the measurements of many NMM also discussed in this paper.

2.3. Gas-Phase Measurements of NMR Frequencies

It is very profitable to perform experiments in the gas phase. Typically, gaseous samples are prepared in the glass vacuum line equipped with a pump, cold traps, and a pressure gauge. Samples are filled with pure gases by condensation in liquid nitrogen or liquid helium temperatures and sealed under a vacuum by a torch. These gas ampoules are fitted into the thin-walled NMR tubes with liquid deuterated solvents in the annular space for use the lock system. In this way, prepared test tubes, after checking its strength, can be measured in most NMR spectrometers, such as conventional liquid samples.

Any given property of a gaseous state in equilibrium can be conveniently expressed as the virial expansion of a power series of the density number [13]. The virial coefficients characterize the isolated molecule $\nu_0(^nX)$ and the intermolecular interactions $\nu_{AB}(^nX)$ between gaseous ingredients at a given temperature. Frequencies extrapolated to the zero-pressure limit are commonly used in this case:

$$\nu(^nX) = \nu_0(^nX) + \nu_{AA}(^nX)\varrho_A + \nu_{AB}(^nX)\varrho_B + \dots . \tag{6}$$

where ϱ_A and ϱ_B are the densities of A and B gaseous substances. The virial coefficients ν_{AA} and ν_{AB} depend on the bulk susceptibility corrections and on the terms involving the intermolecular interactions, which take place during collisions. The amount of A is usually maintained at very low concentrations, and the temperature is kept constant. The above equation can therefore be formulated in a simpler fashion:

$$\nu(^nX) = \nu_0(^nX) + \nu_{AB}(^nX)\varrho_B \tag{7}$$

Analogously, the magnetic shielding parameter $\sigma(X)$ can be written as a simple concentration (density) function; and the equation is valid when chemical shifts δ (ppm) or nuclear magnetic shielding σ (ppm) are analyzed as pressure (density) functions:

$$\sigma(X) = \sigma_o(X) + \sigma_{AB}(X)\,\varrho_B \tag{8}$$

where $\sigma_o(X)$ is the chemical shielding of the X nucleus in the isolated molecule or atom, and σ_{AB} means the second virial coefficient of chemical shielding. The σ_{AB} term is due to bimolecular collisions involving several specific interactions and the bulk susceptibility effect of the gas. At moderate densities, the influence of three-body and high-order collisions can be neglected. In gaseous phases, linear dependencies (7) and (8) are observed up to pressures of ~40 atm [14] where only interactions of two bodies occur. Extrapolation of the shielding values to the zero density limit provides the σ_o, parameter, which is free from intermolecular interactions. It is important to use at least two different gaseous solvents to test the final result of $\sigma_o(X)$; within the limit of experimental error every solvent should give the same value. The $\sigma_o(X)$ constants may be directly compared with the results of quantum chemical calculations for a single molecule or atom in a vacuum (at the temperature of the experiment).

2.4. Diamagnetic Corrections

In the NMR experiment, we can measure the NMM disturbed by the influence of the electron density in the given molecule or atom. These systematic effects, often known as diamagnetic corrections, are expressed as shielding constants σ_X (see Equations (3)–(5)). They describe the magnetic polarization of the medium by an external field. The more accurate corrections are, therefore, necessary to extract the NMM for the bare nuclei. The aforementioned factors should be involved for the reference nucleus and given nucleus under study. Since the first magnetism theories, these correction factors have been called diamagnetic factors. In our case, the diamagnetic factor is a multiplier in Equation (5) defined by means of:

$$f_X = \frac{(1 - \sigma_Y)}{(1 - \sigma_X)} \tag{9}$$

where $\sigma_{X,Y}$ are the shielding of nuclei X and Y, belonging to the reference nucleus and that under consideration. The shielding factors should be expressed on the absolute scale in ppm units. In this case, the diamagnetic shielding factor can appear as close to 1. The f_X factors are shown in tables presented in the next paragraphs. In practice, the correction factor of diamagnetic shielding can even be as large as ~14,000 ppm for ^{185}Re and ^{187}Re, which results in a dipole magnetic moment correction of ~3×10^{-2} μ_N [15]. On the other hand, these corrections in the proton case are of the order 3×10^{-5} ppm. We can suppose that correction factors for a particular noble gas will be of varying importance. The numerical corrections are shown in Table 8, and a short discussion about this problem can be found in the Summary and Prospect part of this paper.

2.5. Direct Measurements of Shielding Constants

A considerable effort has been made to establish the so-called absolute shielding scales for individual active nuclei (e.g., see [15,16]). Generally, good shielding scales are known for ^{1}H [17] and a few light nuclei [18,19]. The worse situations concern heavy nuclei where strong relativistic effects are present. The theoretical calculations of these effects have only been used in the last decade, and a relatively limited quantity of relativistic data has been known up to now. The validity of the shielding corrections rises when atomic numbers increase for the given nuclei. This means that the NMM of heavy isotopes are given with much less accuracy than for light nuclei.

2.6. Other Methods

Several physico-chemical techniques can serve as a source of NMM values: microwave spectroscopy, atomic and molecular beam experiments, optical spectroscopy, optical double resonance and pumping techniques, Mössbauer spectroscopy, nuclear orientation, specific heat measurements, and dynamic nuclear self-polarization. Among them, the atomic and molecular beam resonance methods (ABMR) have played a main role when the NMM of stable nuclei are of interest [20,21]. ABMR is a method related to the well-known NMR spectroscopy technique. Several variations of this approach exist. Atomic or molecular beams are generated in a vacuum line by heating samples to a

high temperature. The beams are then formatted in the high vacuum apparatus where two magnets create inhomogeneous magnetic fields to influence the trajectories of particles before going to the detector. A strong magnetic oscillation field gradient was used to flip the magnetic moment of particles. The selection of quantum states connected with spin magnetic moments through space quantization can give a characteristic pattern of resonance lines. If the resonance condition is fulfilled:

$$\omega_R = \gamma/\hbar \times B_R \tag{10}$$

The spin is now precessing around the B_R direction with an angular frequency known as the Rabi frequency ω_R. The precession rate is independent of the spatial distribution of the spins. The Rabi method was capable of detecting the magnetic resonance absorption spectra and estimating nuclear magnetic moments of several nuclei, among them protons, deuterium, and heavier nuclei [22]. The concept of the ABMR method in the more sophisticated variations can also be used for studying short-lived radioactive nuclei (isotopes with a half-life shorter than 1 min) and metastable states (a life-time of at least a few milliseconds). It is very beneficial when the NMM of nucleus is known from ABMR and NMR methods at the same time because of the possibility of comparing both results for different chemical species and verifying shielding constants and magnetic moments together (see for example [23]).

Many NMMs of short lived nuclides were measured by Collinear Fast Beam Laser Spectroscopy (CFBLS, CLS), Optical Pumping (OP) with Radiative Detection and β-NMR experiments. The CFBLS method is a kind of high resolution laser spectroscopy for investigations of short-lived isotopes in their ground-states. This method was developed by Kaufman [24]. CLS can not only investigate nuclear magnetic moments but also different nuclear properties, such as nuclear charge radii [25]. β-NMR is a general method suited to many fields of research and can measure shifts in the Larmor frequency and relaxation times. The spectroscopic NMR signal is observed as the anisotropic emission of β-particles. It can be prepared for application to the short-lived β decaying nuclei that are delivered as a beam species. Because of the former nuclei hyperpolarization, this method has a sensitivity of even five orders of magnitude more than that of a normal NMR experiment [26,27]. Several examples of these methods of research will be presented in relation to [17]Ne-[27]Ne, [33]Ar-[43]Ar, and [203]Rn-[225]Rn nuclei in the following sections.

The experimental results of NMM measurements for stable isotopes of noble gases performed so far by ABMR and NMR methods were collected in the series of Tables 1, 2, 5 and 6. The original results of individual measurements were recalculated using the new, best quality physical quantities and then included in the tables. The final results are not identical to the author's primary, original findings.

3. Isotopes of Noble Gases and Magnetic Moments

3.1. Helium ($_2$He)

Helium is, after hydrogen, the second lightest and second most abundant element in the universe. Helium has similar behavioral properties to that of an ideal gas and exists as a monoatomic substance. It fulfils the Universal Gas Law with a good approximation. Completely nonreactive, it does not form any known chemical compounds. However, new materials with helium incorporated into the fullerenes were synthesized and spectroscopically investigated [28]. Helium in the Earth's atmosphere is relatively rare, ~5.2 ppm by volume. There are nine isotopes of helium from [2]He up to [10]He, but only two of them are stable: [3]He ($I = 1/2$) and [4]He ($I = 0$) [29]. The isotopic abundance of the first isotope in the Earth's atmosphere is 1.37 parts per million (0.000137%); however, only this nuclide can be applied in NMR measurements.

In the perspective of theoretical physics, He is subject to the laws of quantum statistics; [4]He are bosons but [3]He are fermions. Liquid helium exhibits the strongest quantum effects. Both isotopes play an important role in cryogenic applications as a source of extremely low temperatures. A rare isotope of helium—[3]He, is used as a refrigerator to achieve temperatures of the order of 0.2 to 0.3 K

and in mixtures with [4]He to reach temperatures as low as a few thousands of a kelvin. The boiling points of helium isotopic forms (4.23 K, 3.1905 K for [4]He and [3]He, respectively) are lower than those of any other substance. Commercially, helium-3 is manufactured through the nuclear decay of tritium, a radioactive isotope of hydrogen. The most effective commercial source of helium-3 is the nuclear weapon utilization program in the U.S. [30].

Precise knowledge of the helium-3 NMM is of prime importance because a small nucleus (2 protons and 1 neutron) can be good to test the summation of neutron and proton magnetic moments. This outstanding nucleus has its mirror analog in the tritium nucleus. The nuclear spin of helium-3 (triton) was determined from the intensity alternation in the band spectrum of the helium dimer [31]; the sign of the [3]He nuclear magnetic moment is opposite to that of the proton [32]. Over the last seventy years, several attempts have been made to precisely determine the [3]He nuclear magnetic moment. The first attempt was made by Anderson and Novick in 1949 [33] in an NMR experiment using helium and water H_2O, where the g-factor of [3]He was roughly established as 0.763 of a proton.

All systems under examination, used to establish μ([3]He), are listed in Table 1 [34–42] along with the appropriate diamagnetic corrections and magnetic moments and will be discussed shortly.

Table 1. Nuclear magnetic moment of helium-3 from nuclear magnetic resonance (NMR) spectroscopy.

System	$\dfrac{\nu(^3\text{He})/\nu(^1\text{H})}{\nu(^3\text{He})/\nu(^2\text{H})}$	Correction Factor	$\mu(^3\text{He})/\mu_N$	Reference
[3]He-H_2-O_2	0.7617866(12)	1.000033681	−2.1276253(34)	Anderson, 1949 [34]
[3]He-H_2	0.76178685(8)	1.000033681	−2.12762604(24)	Williams, Hughes,1968 [35]
[3]He-H_2-O_2	0.761786635(4)	1.000033681	−2.12762554(1)	Neronov, Barzakh, 1977 [36]
[3]He-HD-O_2	0.7617866612(45)	1.000033637	−2.12762550(1)	-
[3]He-D_2-O_2	4.962582498(63)	1.000033581	−2.12762542(3)	-
[3]He-H_2O	0.76178632(8)	1.000034279	−2.1276258(3)	Belyi, Shifrin, 1986 [37]
-	0.7617861313(33)	1.000034279	−2.12762530(2)	Flowers, Petley, Richards, 1993 [38]
[3]He-CD_3OD	4.962598074	1.000030376	−2.12762529	Hoffman, Becker, 2005 [39]
[3]He-TMS-	0.76179156(1)	1.000027154	−2.12762531(3)	Jackowski et al., 2008 [40]
c-C_6D_{12}	4.96260924(7)	1.000028135	−2.12762530(3)	-
[3]He-D_2	4.962582261(4)	1.000033581	−2.12762533(1)	Aruev, Neronov, 2012 [42]
[3]He-H_2-CO_2,N_2O, CF_4	0.761786594(5)	1.000033681	−2.127625311(22)	Makulski, [this work]

Anderson attempted the precise measurements of μ([3]He) in a gaseous mixture of [3]He/H_2/O_2 (1/0.37/1 proportion and pressure of 24 atm) and received the result of 0.7617866(13) for the ratio of the frequencies ν([3]He)/ν(^{1}H) [34]. However, the presence of large amounts of paramagnetic oxygen (which can cause a change of local magnetic field) reduced the validity of this experiment, despite good agreement with the next achievements. This result was upgraded to an accuracy of 0.1 ppm by Williams and Hughes [35]—0.76178685. Progress has essentially been achieved in this area because of the efforts Neronov et al. in a series of papers [36,41,42].

Discussion regarding the older results of gas phase experiments in the [3]He/H_2/HD/D_2/O_2 mixtures can be omitted as the presence of large amounts of paramagnetic oxygen ingredients can falsify the final results. Very precise measurements lead to a ratio of [3]He/^{1}H NMR spin precession frequencies 0.761786594(2) in the [3]He/H_2 mixture [41] and to a [3]H_3/^{2}H ratio of 4.962582261(4) in the [3]He/D_2 mixture [42]. The final results of the NMM mentioned above (see Table 1) were corrected by factors that came from shielding parameters of helium-3 σ_0 = 59.96743(10) ppm [43] and from protons in H_2 (26.293(5) ppm) and deuterons in D_2 molecules (26.288(3) ppm)) [17]. For recalculation of the original results, we have used the best known shielding corrections and magnetic moments of proton [44] and deuteron [11] (see Table 1).

More reliable experiments will be those carried out by Flowers, Petley, and Richards [38] in pure helium-3 samples against the proton signal in liquid water. The frequency of optically pumped [3]He nuclei and that of protons in water H_2O were measured in an accurately spherical sample cell in the same magnetic field of 0.1 T and 25 °C. The interchange of sample [3]He and water was carefully

computer controlled. Several corrections of temperature, magnetic field homogeneity, shape correction, and other things were involved. These accurate measurements and new corrections for shielding in water samples (25.691(11) ppm [11]) and that of ^{3}He lead to a final result of $\mu(^3$He$) = 2.127625308(25)\ \mu_N$. The last value was included in the latest collections of fundamental physics constants, namely those recommended by Stone in the "Table of recommended nuclear magnetic dipole moments" published under the auspices of the INDC (International Nuclear Data Committee, November 2019 [45].

Another approach to these studies was made by Jackowski et al. [40] from experiments that related the resonance frequency of the ^{3}He nucleus to the resonance frequency of the ^{1}H nucleus in neat tetramethylsilane (TMS). For the first time, the pressure dependence of ^{3}He chemical shifts was observed in the gaseous phase and the radiofrequency for the isolated helium atom was given. The shielding correction in liquid TMS was then applied as σ (^{1}H, TMS) = 32.815(5) ppm [17], and in liquid cyclohexane-d$_6$ as σ (^{2}H, (CD$_2$)$_6$) = 31.834 ppm [46].

For purpose of this work, new experiments in gaseous H$_2$/^{3}He mixes were performed. Namely, three different mixtures were examine—^{3}He/H$_2$ in CO$_2$, N$_2$O, and CF$_4$ as buffer gases to measure the frequency ratio of ^{3}He/^{1}H in the zero-pressure limit (see Figure 1). To fulfill Equation (8) the minor components in gas mixtures (^{3}He-H$_2$) were maintained at small concentrations less than 5×10^{-3} mol/L. CO$_2$, N$_2$O, and CF$_4$ buffer gases were used in much excess. All data points are from single measurements of one dimensional NMR spectra. The density function plots were analyzed according to the Equation (7). Only in this case are the diamagnetic corrections adequate in the theoretical results for molecules in a vacuum—for the isolated He atom and H$_2$ molecules at a given temperature of 300 K.
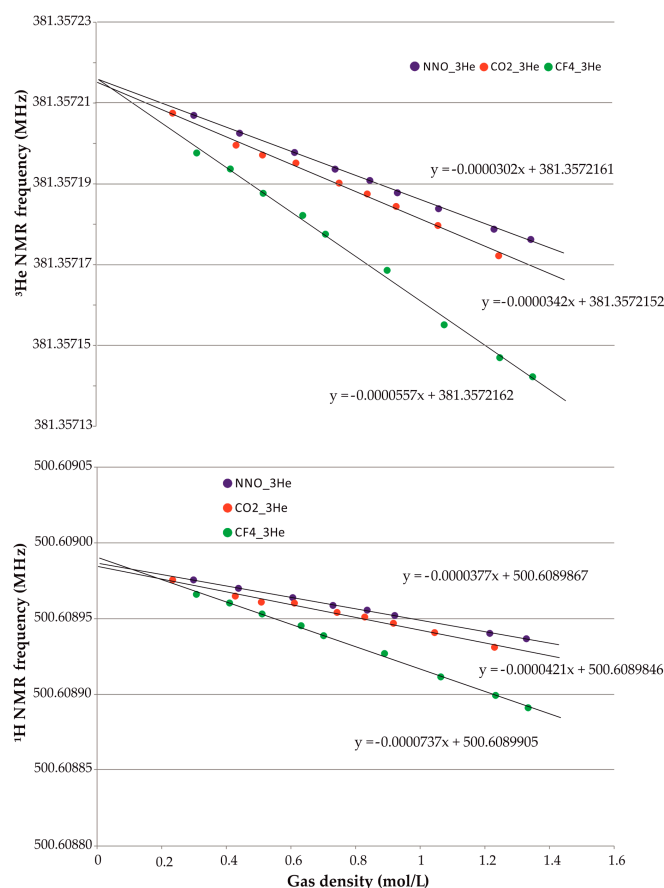

Figure 1. ^{1}H and ^{3}He NMR frequencies recorded in ^{3}He/H$_2$ mixture immersed in buffer gases: CF$_4$, CO$_2$, and N$_2$O.

The extrapolated average frequencies are as follows: $\nu(^1\text{H}) = 500.6089872(17)$ and $\nu(^3\text{He}) = 381.3572158(5)$ MHz. The appropriate shielding correction was applied to establish the final result for bare nuclei. All calculated helium-3 magnetic moments from experiments with different buffers were from $-2.127625286(15)$ up to $-2.127625333(16)$ μ_N, in agreement with the previously reported results. At this high precision, the calculations for all component errors are important. However, the main source of error originates from the proton shielding correction factor in the H_2 isolated molecule [17].

In summary, we can ascertain that the helium-3 dipole moment belongs to the more precise values established for any nucleus in the periodic table apart from proton and deuteron. It is important that helium atoms can be used in different gaseous mixtures for comparative NMMs measurements of other nuclei. All results from the experimental observations up to now are schematically shown in Figure 2.
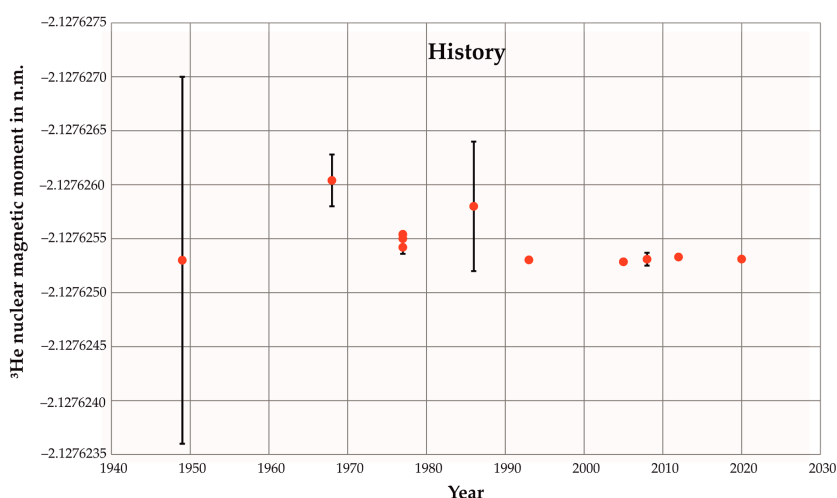

Figure 2. The nuclear magnetic moment of ^{3}He measured by the NMR method.

The tendency for the stable NMM results around the value $2.1276263\mu_N$ has been accomplished over time and is clearly visible. Good agreement between the old result of Anderson (1949) and more recent ones (2008, 2012, and 2020) can be of accidental origin when errors and approximations cancel each other out. Only the extrapolated parameters and shielding corrections for isolated atoms or molecules are methodologically correct. The above results show that NMR spectroscopy has reached its limit for further improving the results using the standard NMR method in this case. The other advanced physical methods could lead to radical progress in the future.

3.2. Neon ($_{10}$Ne)

Neon is the fifth most abundant element in the universe (fourth according to the Jefferson Laboratory). It is present in the Earth's atmosphere at 0.0018% by volume, and is lighter than air. Liquefied is an important cryogenic refrigerant. It is commercially available from the fractional distillation of liquid air. Interestingly, neon was the first element recognized as a mixture of three stable isotopes. It consists of three stable isotopes: ^{20}Ne (90.48%), ^{21}Ne (0.27%), and ^{22}Ne (9.25%) [29]. ^{22}Ne is used for the production of radioisotope ^{22}Na in medical treatment and ^{20}Ne is a precursor of ^{18}F used in the radiopharmaceutical industry. Only Ne-21 ($I = 3/2$), apart from maser building, can be used to study the NMR resonance. Unfortunately, the nucleus—^{21}Ne possesses quite a large quadrupole moment Q = 0.10155(75) barn [45] but in a very symmetrical environment, the resonance lines are expected to be not too wide. Neon forms no chemical compounds.

^{21}Ne NMM was measured for the first time by LaTourette et al. against the deuterium signal of D_2 [47] in an ABMR experiment. The original value of the NMM was $-0.661758(5)$, and this was recalculated using the new magnetic shielding coefficient $\mu(^{21}\text{Ne}) = -0.6617895$ μ_N. This value

was recently measured by NMR spectroscopy performed in the gas state on neon gas at the natural abundance: −0.6617774(10) [48]. The pressure dependence of NMR frequencies was determined in the density range 0.13–2.90 mol/L. This function shows a strictly linear dependence. The ^{21}Ne frequency results were compared with those for the ^{1}H frequency of the residual signal of benzene-d$_6$ used as a "lock" reference.

We cannot use helium-3 to measure the NMM of neon-21 because its low resonance frequency means that neon measurements must be made on a low band probe where the frequency of helium-3 cannot be achieved. The second reason for this not being possible was the fact that large glass ampoules with 8 mm o.d. not suited to the helium measurement probe had to be used. Instead of this, we chose the residual signal of ^{1}H and ^{2}H(D) resonance frequencies as reference nuclei of the lock system (see Table 2). The main source of the shielding factor correction is for the neon isolated atom. Its magnetic shielding can certainly be taken from chemical quantum calculations. They are in the range of 561.3–556.83 [48]. We chose the recently calculated result of 557.1123 ppm by the four-component relativistic method [49]. Finally, it can be seen that both experimental techniques, ABMR and gas phase NMR, lead to practically the same result, which only varies by 0.016% (see Table 2).

Table 2. Parameters for establishing of the neon-21 nuclear magnetic moment.

Method/System	$\nu(^{21}Ne)/\nu(^nX)$	Correction Factor	$\mu(^{21}Ne)/\mu_N$	Reference
ABMR method ^{21}Ne-D$_2$	$\nu(^{21}Ne)/\nu(^2H)$ 0.514274(4)	1.000531020	−0.661789(5)	LaTourette, Quinn, Ramsey, 1957 [47]
free precesion ^{21}Ne-^{3}He	$\nu(^{21}Ne)/\nu(^3He)$ 0.10364(1)	1.000497422	−0.66184(7)	Chupp, Oteiza, Richardson, 1988 [50]
NMR method ^{21}Ne-C$_6$D$_5$H	$\nu(^{21}Ne)/\nu(^1H)$ 0.078942872(2)	1.000531065	−0.6617774(10)	Makulski, Garbacz, 2020 [48]
^{21}Ne-C$_6$D$_6$	$\nu(^{21}Ne)/\nu(^2H)$ 0.514265413(6)	1.000530967	−0.6617774(10)	-

The noble-gas polarization technique of spin exchange with laser optically pumped Rb allows several noble gases to be polarized simultaneously, among them helium-3 and neon-21 and the free resonance frequency to be observed [50]. A rather large error in frequencies gave the NMM of neon-21 with limited precision.

The theoretical physical attempts to calculate $\mu(^{21}Ne)$ provided several, slightly different values: 0.660, 0.774, 0.824, 0.741, and 0.688 in nuclear magnetons, depending on the method used [51]. Using the example of neon, we are able to discuss the NMM measurements of short-lived nuclei from the fast-beam collinear laser spectroscopy method [52]. In addition to the NMMs, there are other important physical properties that describe the form of particular nuclei: quadrupole electric moments (in barn, 1b = 10^{-28} m^2) and mean square charge radii. Both electromagnetic moments for different neon isotopes [53], among them unstable nuclei, are shown in Table 3.

Table 3. Electromagnetic properties of neon isotopes [53] *.

Nuclide	I^π	Abundance (%)	$T_{1/2}$	Q/barn (10^{-28} m^2)	Method	μ/μ_N	Method
^{17}Ne	1/2$^-$	-	109.2 ms	-	-	+0.7873(14)	CFBLS
^{19}Ne	1/2$^+$	-	17.34 s	-	-	−1.88542(8)	β-NMR
^{20}Ne	-	90.48	-	-	-	-	-
^{21}Ne	3/2$^+$	0.27	stable	0.10155(75)	O/AB	−0.661797(5)	MB
^{22}Ne	-	9.25	-	-	-	-	-
^{23}Ne	5/2$^+$	-	37.24 s	0.145(5)	CFBLS	−1.0817(9)	β-NMR
^{25}Ne	1/2$^+$	-	602 ms	-	-	−1.0062(5)	CFBLS
^{27}Ne	(3/2$^+$)	-	31.5 ms	-	-	-	-

* CFBLS: Colinear Fast Beam Laser Spectroscopy, O/AB: Optical Spectroscopy/Atomic Beam Magnetic Resonance, and MB: Molecular Beam Magnetic Resonance.

3.3. Argon ($_{18}$Ar)

After nitrogen and oxygen, argon gas is the third most abundant component in dehydrated atmospheric air. Argon has 24 known isotopes from ^{30}Ar up to ^{53}Ar but only three of them are stable: ^{36}Ar (0.3365(30)%), ^{38}Ar (0.0632(5)%), and ^{40}Ar (99.6003(30)%) [29]. Unfortunately, none of them are magnetically active. Three other isotopes are relatively long-lived: ^{39}Ar (with a half-life of 269 years), ^{42}Ar (32.9 years), and ^{37}Ar (35.04 days). Almost all argon on Earth comes from the short living ^{40}K (0.012% of natural potassium) isotope in a series of nuclear transformations. Isotopes ^{37}Ar and ^{39}Ar can potentially be used in NMR experiments. The second one is an especially promising experimental object.

The content of ^{39}Ar in natural argon is only 8×10^{-16} g/g, and it comes from the cosmogenic reaction from ^{40}Ar in the upper atmosphere. These radionuclide form in the atmosphere through the nuclear reaction ^{40}Ar(n,2n)^{39}Ar and decay by beta emission to ^{39}K with a half-life of 269 years [54]. We propose using this isotope in the NMR exploration of argon chemical shifts in the future, while carefully considering radioactive material. The nuclear magnetic properties are known: $I = 7/2$ and $\mu(^{39}$Ar$) = -1.588(15)$ [55].

It is possible to predict other NMR quantities—chemical shift range from −110 up to 0.0 ppm, relative resonance frequency Ξ = 8.1222%, line width ~4 Hz and receptivity relative to ^{1}H ~1×10^{-16} [56]. Argon magnetic properties were very rarely a research subject in the literature. For this reason, the ab initio calculations of intermolecular interactions in ArAr, ArNaH, and ArNe systems carried out by Jameson et al. [57] are of prime importance in this field. A few basic properties of argon isotopes are shown in Table 4. The magnetic and quadrupole moments were measured by NMR of beam polarized nuclei with β asymmetry detection (β-NMR), collinear fast beam laser spectroscopy with β detection (CFBLS/ β-NMR), and optical pumping with radiative detection (OP/RD) [58].

Table 4. Argon nuclides and their physicochemical properties *.

Nuclide	I^π	Abundance (%)	Half-Life	Q/barn (10^{-28} m^2)	Method	μ/μ_N	Method
^{33}Ar	1/2$^+$	-	173.0(20) ms	-	-	−0.723(6)	CFBLS/β-NMR
^{35}Ar	3/2$^+$	-	1.775(4) s	0.084(7)	CFBLS/β-NMR	+0.6322(2)	β-NMR
^{36}Ar	-	0.334%	stable	-	-	-	-
^{37}Ar	3/2$^+$	-	35.04(4) d	0.0762(16)	CFBLS/β-NMR	+1.145(5)	NMR, OP/RD
^{38}Ar	-	0.063%	stable	-	-	-	-
^{39}Ar	7/2$^-$	-	269(3) y	0.117(20)	CFBLS/β-NMR	−1.588(15)	CFBLS/β-NMR
^{40}Ar	-	99.604%	stable	-	-	-	-
^{41}Ar	7/2$^-$	-	109.61(4) min	0.042(1)	CFBLS	−1.310(8)	CFBLS
^{43}Ar	5/2$^-$	-	5.37 min	0.142(14)	CFBLS	−1.021(6)	CFBLS

* CFBLS: Colinear Fast Beam Laser Spectroscopy, OP/RD: Optical Pumping with Radiative Detection.

3.4. Krypton ($_{36}$Kr)

The Earth's atmosphere contains about 1.14 ppm of krypton by volume and 10 ppt in the Earth's crust. It is used commercially and is easily separated from liquid air by fractional distillation. Naturally occurring krypton is composed of five stable isotopes: ^{80}Kr (2.286%), ^{82}Kr (11.593%), ^{83}Kr (11.500%), ^{84}Kr (56.987%),^{86}Kr (17.279%), and ^{87}Kr (0.355%) with a very long half-life of 9.2×10^{21} years. Additionally, about 30 unstable isotopes and isomers are known among them ^{85}Kr with a long half-life of 10.776 (3) years [59]. This last isotope is produced in nuclear reactors and power plants. In the atmosphere, it is monitored as a good source of information regarding the consumption of nuclear material in a given area. Krypton can form nothing but a few simple compounds with other atoms under extreme conditions: KrF$_2$, KrF, KrXe, HKrCN, HKrC≡CH, and Kr(H$_2$)$_4$ [60]. Only krypton difluoride, a strong oxidizer, has been synthesized in gram quantities using several methods.

^{83}Kr as the only naturally occurring and magnetically active krypton nucleus with the spin number $I = 9/2$ was used in common NMR investigations in the gaseous state and in solutions. It deviates slightly from the spherical symmetry and should be described as a deformed nucleus that manifests

itself with a relatively high electric quadrupole moment $Q = +0.259 \times 10^{-28}$ m^2 (0.259 barn) [45]. The nucleus ^{83}Kr has 36 protons and 47 neutrons and is notable for its one high spin orbital, 1g$_{9/2}$.

For the first time, the $\mu(^{83}\text{Kr})$ was measured using the ABMR method [61], but with rather limited precision. Afterward, NMR investigations gave more accurate results: $\mu(^{83}\text{Kr}) = -0.9707295\mu_N$ [62] and $\mu(^{83}\text{Kr}) = -0.967221$ μ_N [63]. The ^{3}He and ^{83}Kr NMR frequencies were only recently measured using an advanced technology pulse FT spectrometer in ^{3}He/Kr gaseous mixtures at different densities [64]. Selected krypton spectra are shown in Figure 3. The frequency dependences were analyzed according to Equation (8). The density shift was measured per concentration unit as $\sigma_1(\text{Kr},\text{Kr}) = -3259.1(300)$ ppm ml mol^{-1}. The difference between low and high pressures attains a few ppm and cannot be ignored if shielding corrections are to be properly included. The final result completed against the helium-3 moment is $-0.9707297(32)$ μ_N and remains in excellent agreement with the previous result of Brinkmann et al. [63].
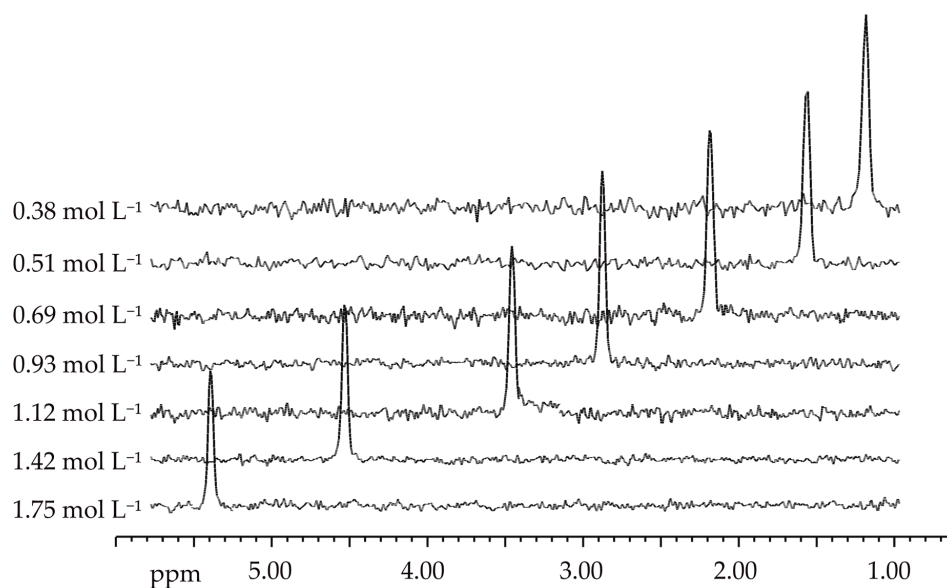

Figure 3. The series of ^{83}Kr NMR spectra measured at different krypton densities in the range $0.38 \div 1.75$ mol/L at 300 K. A valuable density shift is clearly visible.

In addition to the magnetic moment for the $I = 9/2$ ground state ^{83}Kr nucleus, the magnetic moment of the metastable krypton ^{83m}Kr (half-life 1.83 h) nucleus was measured by collinear fast-beam laser spectroscopy in arrangement with sensitive collisional ionization detection [65]. The short lived isomeric state ^{83m}Kr ($I = 1/2^-$) excited at 41.55 keV can be generated from the radioactive ^{83}Rb source (T$_{1/2}$ = 86.2 d). The difference between the NMM in the ground and the first excited state is valuable and equals 1.562 μ_N (see Table 5).

Table 5. Experimental data for evaluation of ^{83}Kr magnetic moment.

Method/System	$\nu(^{83}\text{Kr})/\nu(^n\text{H})$	Correction Factor	$\mu(^{83}\text{Kr})$ μ_N	Reference
ABMR Kr	-	1.0035773	−0.9700	Kellog, Millmann, 1946 [61]
NMR Kr-H$_2$O	0.0384825(6)	1.0035644	−0.970729(20)	Brinkman, 1968 [62]
NMR Kr-H$_2$O	0.0384825(6)	1.0035644	−0.970730(15)	Brinkmann, 1968 [63]
NMR Kr-^{3}He	$\nu(^{83}\text{Kr})/\nu(^3\text{He})$ 0.0505161561(3)	1.00352996	−0.9707297(32)	Makulski, 2014 [64]
85^{m}Kr	-	-	+0.591(2)	Kleim et al., 1995 [65]

3.5. Xenon ($_{54}$Xe)

At standard conditions (temperature and pressure) gaseous xenon has a density of 5.761 kg/m^3. Xenon can be liquefied at −111.7 °C (161.4K). Surprisingly, in the liquid state xenon possesses high polarizability and can be a good solvent for many hydrocarbons and even water. It is found in the Earth's atmosphere at a concentration of 8.7 ppb by volume. Generally, it is unreactive but can form many stable compounds, mainly with strong electronegative elements, such as fluorine and oxygen: XeF_2, XeF_4, $XeOF_2$, XeF_6, XeO_4, H_6XeO_6, $XePtF_6$, and many ionic species in water solutions [66]. NMR spectroscopy of xenon is, therefore, an interesting and still progressive field of spectroscopy [67]. Xenon is obtained commercially by extraction from liquid air.

A naturally occurring element, it consists of seven stable isotopes: ^{126}Xe (0.089%), ^{128}Xe (1.910%), ^{129}Xe (26.401%), ^{130}Xe (4.071%), ^{131}Xe (21.232%), ^{132}Xe (26.909%), and ^{134}Xe (10.436%). A few other isotopes are long lived: ^{124}Xe (0.095%, 1.8x1022y), ^{125}Xe (16.9 h), ^{127}Xe (36.345 d) and ^{133}Xe (5.247 d), ^{135}Xe (9.14h), and ^{136}Xe (8.857%, 2.165×10^{21} y) [29]. In the magnetic resonance method, two nuclides of natural abundance can be utilized: ^{129}Xe (with 75 neutrons) with the spin number $I = 1/2^-$ and ^{131}Xe (with 77 neutrons) with $I = 3/2^+$.

Kopfermann et al. determined from the hfs (hyperfine structure) measurements that the former has a spin of 1/2 and the latter a spin of 3/2 [68]. The receptivity of the ^{129}Xe nuclei is 5.72×10^{-3} of that of a proton and encompasses a large spectral range of 5800 ppm due to its extreme sensitivity to the different chemical environments. Interestingly, the lower sensitivity nucleus ^{131}Xe, which is quadrupolar, can show additional signals in the gas phase when gas-solid glass ampoule collisions take place. This behavior is depicted in Figure 4a along with the analogous signal of ^{129}Xe, which has $I = 1/2$ and no quadrupole moment (Figure 4b). Gas-phase ^{131}Xe atoms exhibiting nuclear quadrupole interactions with the surface of the glass samples were observed earlier and explained by the model of atoms absorbed on surfaces (see for example [69]) and high magnetic field strength [70].
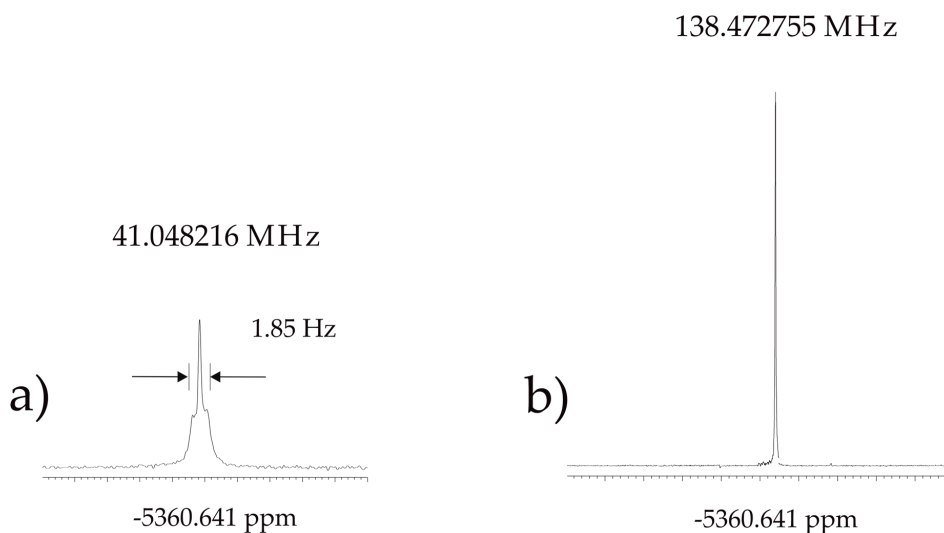

Figure 4. (**a**) ^{131}Xe and (**b**) ^{129}Xe NMR signals from gas phase measurements at 31.51 atm (1.3 mol/L) and magnetic field 11.75 T. Specific additional splitting in the ^{131}Xe resonance is clearly visible.

One of the first measurements of the NMM was performed by Proctor and Yu [71] for a number of nuclei, including for ^{129}Xe. Brun et al. [72] measured both xenon active isotopes a few years ago with much more precision in pure gas at approximately 50 atm. against that of protons in water containing 0.1 M $MnSO_4$ as the relaxation reagent. It was seen that the chemical shift/frequency of xenon resonances were strongly dependent on the gas density, which reinforced the measurements in the series samples of different pressures.

Brinkmann [73] measured the NMM of xenon isotopes taking the deuteron nucleus in heavy water, with small amounts of $FeCl_3$ as a relaxation agent, as a reference standard. However, the use of paramagnetic substances can modify the final result to the same extent. The next attempt to better establish the ^{129}Xe magnetic moment took place when Pfeffer and Lutz [74] made their experiments in xenon dopped oxygen to shorten the rather long relaxation times. They received an impressive precision result of 0.2766027337(30). The usage of oxygen ingredients can also slightly mangle the final number. All the above results of measurements are shown in Table 6.

Table 6. Experimental parameters for measuring xenon nuclear magnetic moments.

Method/System	$\nu(^{129}Xe)/\nu(^{n}X)$	Correction Factor	$\mu(^{129}Xe)/\mu_N$	Reference
NMR/Xe-^{23}NaCl	1.0457(1)	not used	−0.7726(1)	Proktor Yu, 1951 [71]
NMR-Xe-H_2O	0.276633(5)	1.007057226	−0.778046(22)	Brun, Oeser, Staub, Telschow 1954 [72]
NMR/Xe-D_2O	1.80192(2)	1.007057226	−0.777969(9)	Brinkmann, 1968 [73]
NMR/Xe-H_2O	0.276602734(3)	1.00705725	−0.777961(6)	Pfeffer, Lutz, 1993 [74]
NMR/Xe-^{3}He, Xe-He-SF_6/CO_2	0.363097481	1.007022726	−0.7779607(80)	Makulski, 2014 [75]
SQUID/Xe-^{3}He-N_2	0.363097288	1.007022726	−0.7779603(78)	Fan et al., 2016 [76]
Method/System	$\nu(^{131}Xe)/\nu(^{n}X)$	**Correction Factor**	$\mu(^{131}Xe)/\mu_N$	**Reference**
NMR-Xe-H_2O	0.081976(1)	1.007057226	+0.691687(17)	Brun, Oeser, Staub, Telschow 1954 [72]
NMR/Xe-D_2O	0.534155(3)	1.007057226	+0.691856(4)	Brinkmann, 1968 [73]
NMR/Xe-He, Xe-He-SF_6/CO_2	0.107634919	1.007022726	+0.6918451(70)	Makulski, 2014 [75]

The author's latest work on this topic was published recently on experiments free of methodological limitations [75]. Small amounts of ^{3}He or ^{3}He/Xe mixture ($\leq 3.0 \times 10^{-3}$ mol/L, pressure ~80 mmHg) as the solutes and pure Xe or SF_6 and CO_2 gases were taken as the buffers. They were analyzed in ^{3}He and ^{129}Xe NMR spectra at the external field, $B_0 = 12.7586$ T. In each case, the resonance frequencies (ν^{He} and $\nu^{129,131}$Xe) were linearly dependent on the total density of the xenon gas. Extrapolation to the zero-density limit allowed these frequencies to be evaluated as free from intermolecular interactions. Combining these values with the recommended σ ($^{129/131}$Xe) and σ (^{3}He) nuclear magnetic shielding constants led to the following final results: $\mu(^{129}Xe) = -0.7779607(158)$ μ_N and $\mu(^{131}Xe) = +0.6918451(70)$ μ_N.

In our opinion, these are the best results known up to now for both xenon magnetic moments. A direct and precise determination of ^{3}He/^{129}Xe was performed recently in a comagnetometer setup under an ultralow ambient magnetic field ($0.4 < \mu_T$) [76]. From the ratio of $\gamma(He)/\gamma(Xe)$, the magnetic moment of ^{129}Xe was obtained as −0.77796029(2) μ_N, which is in very good agreement with our former result. The ratio of two different xenon magnetic moments can be given as 1.1244724, which is in accord with our measured ratio 1.12447237.

3.6. Radon ($_{86}$Rn)

Radon is a naturally-occurring chemical element as an α,β-radioactive gas. It is produced as an intermediate step in the radioactive decay chain of radium ($T_{1/2}$ ~1600 years). As it is a final radionuclide of the decay chain of thorium and uranium (two of the most common radioactive elements on Earth, which have three isotopes with very long half-lives), it is seen in many places as it is a continually generated natural substance. It is nonreactive chemically and, therefore, does not form chemical compounds. Radon concentrations in the atmosphere are too low to be measured by standard chemical methods. However, a few reports on the existence of compounds involving oxygen and fluorine bound to radon have occurred.

At present, there are 35 known isotopes of radon, and all are radioactive [29]. The most stable is the ^{222}Ra isotope with a half-life of 3.823 days. Two other isotopes occur in nature: ^{219}R and ^{220}Ra with a half-life of less than 1 min. A few other isotopes exist in trace quantities as decay products or

as intermediates in the decay chain of different heavier isotopes. The most favorable conditions of NMR measurements belong to ^{211}Rn with a half-life 14.6 h and spin number 1/2. The nuclear magnetic moment of this isotope was established as $\mu(^{211}\text{Rn}) = 0.601(7)\mu_N$. The nuclear moments—both magnetic dipole and electric quadrupole—belong to odd mass numbers of radon. They were established formerly by the spin-exchange optical pumping method [77]. Selected nuclear properties of radon isotopes are shown in Table 7.

Table 7. Electromagnetic properties of radon isotopes.

Isotope	Half-Life	Spin	μ_X/μ_N	Q/barn
^{203}Rn	26.9 s	$13/2^+$	−0.9555(18)	1.28(13)
^{205}Rn	170(4) s	$5/2^-$	+0.7980(16)	0.062
^{207}Rn	9.25(17) m	$5/2^-$	+0.8124(16)	0.22
^{209}Rn	28.8(10) m	$5/2^-$	+0.8348(12)	0.311
^{211}Rn	14.6(2) h	$1/2^-$	+0.5984(12)	-
^{219}Rn	3.96(1) s	$5/2^+$	−0.4399(12)	1.15
^{221}Rn	25 m	$7/2^+$	−0.0201(6)	−0.38
^{222}Rn	3.8235(3) d	-	-	-
^{223}Rn	24.3(4) m	$7/2^-$	−0.772(8)	0.8
^{225}Rn	4.66(4) m	$7/2^-$	−0.693(8)	0.85

3.7. Oganesson ($_{118}$Og)

Oganesson is a radioactive, short lived element produced artificially. It was discovered in 2002 at the Institute for Nuclear Research in Dubna-Russia [78]. The only known isotope is ^{294}Og with a half-life of ~0.89 ms. It possesses the highest atomic number and atomic mass of all known elements. Up to now, the oganesson isotope has only been synthesized in a few atoms; therefore, the chemical properties of this element have not been experimentally evaluated. The electromagnetic properties can only then be known from theoretical predictions, which are still scarce. The expected chemical properties following the periodic trends indicate a large polarizability, two times that of radon and slightly more reactivity than radon. Theoretical calculations have shown that other isotopes, 293, 295, 296, 297, 298, 300, and 302, can be even more stable than the 294 isotope mentioned above. Some of them can potentially have a non-zero spin and nuclear magnetic moment.

3.8. Theoretical Calculations of NMMs

At the end of our considerations, it is necessary to mention the pure theoretical achievements in the field of nuclear magnetic moment calculations. The experimentally measured moments are "highly sensitive to the underlying structure of atomic nuclei and, therefore, serve as a stringent test of nuclear models" [6]. In the past decades, the different theories of nuclear structure were developed starting from the single particle shell model up to the covariant DFT (Density Functional Theory) model, incorporating relativistic effects with several additional corrections e.g., one-pion exchange-current.

Several semi-empirical calculated results for the helium-3 nucleus were discussed in factor g_I terms: $g_I(^3\text{He}) = -3.826$ (Schmidt line), $g_I(^3\text{He}) = -4.255$ (EV,FT) and $g_I(^3\text{He}) = -4.220$ (full-scale shell) compared with the experimental value of $g_I(^3\text{He}) = -4.2552506(1)$ [79]. On the other hand, the best result in the quark model gave the values $g_I(^3\text{He}) = -4.009828$, $g_I(^3\text{He}) = -3.826084$ in the shell model, $g_I(^3\text{He}) = -4.5810$ in the QCD (Quantum Chromodynamics) model [80] and $g_I(^3\text{He}) = -4.16$ in the effective field theory (EFT) of short range interactions [81].

Even in the case of helium, a very simple nucleus, the precision and accuracy of the theoretical predictions is far from those of experimental achievements. This statement is valid for all nuclei in the periodic table, and for all nuclei of remaining noble gases. Nuclear theories have a limited ability to make precise calculations. For readers interested in these problems, the following papers are recommended: for ^{21}Ne calculations [82], and for xenon nuclei [79].

4. Summary and Prospects

"Need for remeasurements of nuclear magnetic dipole moments"—is the title of the paper in the Physics Review that was published by Swedish physicists from Goteborg University more than twenty years ago [83]. This sentence is still valid today. Nuclear magnetic moments are a research subject of Physics and also the chemist community. This is why there have been several controversies and misunderstandings. Nuclear magnetic moments are the basic magnetic properties of nuclei, which include stable, unstable, and in excited states. In a natural way, they are of interest to different scientific groups that use different research techniques. The results of the findings are of prime importance for physical theories of atomic nuclei.

NMR spectroscopy has become the main source of knowledge regarding nuclear magnetic moments of stable nuclei with nonzero spins. This technique as a resonance method can measure resonance frequencies with unprecedented precision, which is the basis of the extraordinary results of nuclear properties. In this work, we provided NMR measurements carried out very recently in the gas phase. Gas phase experiments have important consequences; they give information on diamagnetic corrections suited for determination moments that are free of intra and intermolecular interactions.

The measurements performed in high magnetic fields are accessible in many chemical laboratories today. Additionally, the complemented, high sophisticated quantum-chemical calculations are both necessary and possible. Fortunately, this part of NMR spectroscopy has made outstanding progress in recent years. Using both kinds of data—theoretical and experimental—the NMM of bare nuclei of noble gases were established. The main sources of uncertainty with regard to these values are the shielding correction factors. Table 8 shows the actually preferred results of the NMM of noble gases (He, Ne, Kr, and Xe) calculated using the NMR method along with those established by other methods, suitable for short-lived isotopes (Ar and Rn). The additional data important from a spectroscopic point of view, like spin numbers, magnetic susceptibility [84] and quadrupole moments, is also included. The shielding effects used for corrections of measured magnetic moments are also provided [43,49,85,86]. They were calculated using relativistic methods which show their gain in importance with the mass of noble gas, starting from 59.97 (^{3}He) up to 19630 ppm (Rn). It proves that errors in establishing nuclear moments are in the same direction. The nuclear magnetic moments are shown as $\mu(X)$ value in nuclear magnetons μ_N, g_X factor and $\gamma(X)$ gyromagnetic ratio. All these forms of nuclear magnetism are handled in different fields of chemistry and physics.

Table 8. Preferred values of electromagnetic properties of noble gas nuclei.

Noble Gas Isotope	I^π	Magnetic Susceptibility χ(ppm cm^3 mol^{-1})	Nuclear Magnetic Moment (NMM) (μ/μ_N)	Diamagnetic Correction Factor $(1-\sigma_X)$	g_I Factor	Magnetogiric Ratio ($\gamma \times 10^7$/radT^{-1}s^{-1})	Qudrupole Moment Q(barn) [45]
^{3}He	1/2$^+$	−2.02	−2.127625311(15) [this work]	0.99994003257 [43]	−4.25525062(5)	−20.3801680(2)	-
^{21}Ne	3/2$^+$	−6.96	−0.6617774(10) [48]	0.9994428877 [49]	−0.441185(2)	−2.1130183	0.10155(75)
^{39}Ar	7/2$^-$	−19.32	−1.588(15) [55]	0.9987253 [85]	−0.4537(44)	−2.1317(20)	0.117(20)
^{83}Kr	9/2$^+$	−29	−0.9707297(32) [64]	0.9964227 [85]	−0.2157177(7)	−1.033162(3)	0.259(1)
^{129}Xe	1/2$^+$	−45.5	−0.7779607(158)	0.9929667	−1.55592(2)	−7.451956(75)	-
^{131}Xe	3/2$^+$	-	+0.6918451(70) [75]	[86]	+0.461230(5)	+2.209023 (11)	0.114(1)
^{211}Rn	5/2$^-$	N/A	+0.5984(12) [77]	0.98037 [80]	+0.2394(5)	+2.8660(115)	0.190(2)

Commonly, the NMM are of small quantities ranging from −1.5 up to +1.2μ_N, independent of the number of protons. For noble gas nuclei, the protons are even and fill the levels as paired nucleons—2, 10, 18, 36, 54, and 86 in the shell nuclei model. On the other hand, the neutron presence can change the corresponding NMM of the entire nucleus. The dependence between moments and numbers of neutrons for the noble gases Ne, Ar, Kr, Xe, and Rn is shown in Figure 5. The strong irregularities and sometimes non-monotonic variations for specific isotopes are clearly visible. This rather complicated behavior can be explained in a controversial manner in terms of nuclear rotations and the charge/mass ratio (Q/M) [87].
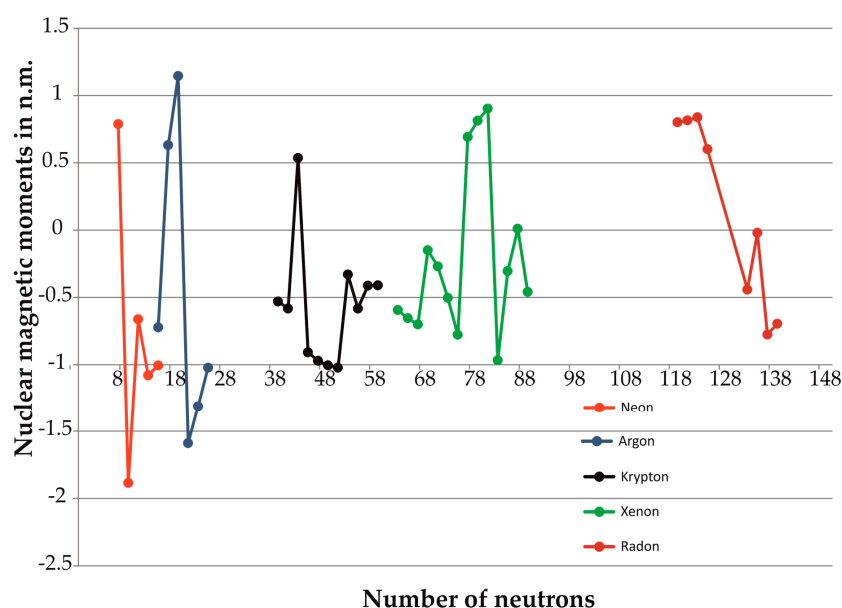
Figure 5. The nuclear magnetic moments plotted versus the number of neutrons in the nuclide.

The nuclear magnetic moments of noble gases are well established when compared with other nuclei in the periodic table. This is a result of extensive gas phase NMR measurements and quantum theoretical calculations of shielding corrections. The first exponent of noble gases—the ^{3}He nucleus has its own central status because we can use the gaseous helium substance in other gaseous mixtures as a convenient reference nuclei in NMR experiments (see Sections 3.4 and 3.5). It is one of the best known moments among nuclei in the all periodic table. The suggested value is 2.127625308(25) μ_N, which was very recently tabulated by Stone in the "Table of recommended nuclear magnetic dipole moments" under the auspices of the INDC International Nuclear Data Committee, November 2019 [39].

The magnetic moment of helion in a helium atom was corrected using the shielding of ^{3}He by its two electrons computed by Rudziński et al. [43] to be $\sigma_0(^3\text{He})$ = 59.96743(5) ppm, the best known shielding constant of any nuclei in any species. Gaseous helium-3 was safely used in many gaseous mixtures and water solutions for determining other NMMs or confirmation of shielding constants, e.g., $^{6/7}$Li, $^{10/11}$B, ^{13}C, ^{23}Na, ^{31}P, $^{35/37}$Cl, and ^{183}W.

Further improvement of the accuracy and precision of the helium-3 nucleus cannot be accomplished using the classic NMR spectroscopy method, but can be expected from new physical methods e.g., in quantum-jump spectroscopy in advanced Penning-trap systems. The success of recent experiments for single isolated protons and antiprotons in CERN's BASE program may open new horizons for the research of other light nuclei. The technical conditions for ^{3}He^{2+} particles have already been proposed by Mooser et al. at RIKEN (Institute of Physical and Chemical Research) EEE Pioneering Project Funding [88].

One of the serious limitations of NMR achievements is the general lack of sensitivity related to low nuclear spin polarization in the sample. Another method of upgrading measurements can be applied by using the hyperpolarized noble gases where strong amplification (up to thousand times) of the signal to noise ratio can be accomplished [89]. This method is troublesome because additional actions for cleaning the system of alkali metals is needed. The great success of the ^{129}Xe NMR-based biosensing approach has been proven with open opportunities of long time monitoring of different biological objects [90].

Finally, we mention the special character of noble gases as magnetic probes in new branches of chemistry [91]. Rare gas atoms can be encapsulated in different kinds of fullerenes and analyzed using diagnostic techniques, among them the NMR spectroscopy method, in particular.

Conflicts of Interest: The author declares no conflict of interest.

References

1. Grochala, W. On the position of helium and neon in the Periodic Table of Elements. *Found. Chem.* **2018**, *20*, 191–207. [CrossRef]
2. Schrobilgen, G.J. Noble gas. In *Encyclopedia Britannica*; Encyclopedia Britannica Inc.: Chicago, IL, USA, 2019; Available online: https://www.britannica.com/science/noble-gas (accessed on 23 October 2020).
3. Grochala, W.; Khriachtchev, L.; Räsänen, M. Noble-gas chemistry. In *Physics and Chemistry at Low Temperatures*, 1st ed.; Khriachtchev, L., Ed.; Taylor &Francis: New York, NY, USA, 2011; Chapter 13; pp. 419–446. [CrossRef]
4. Antušek, A.; Jackowski, K.; Jaszuński, M.; Makulski, W.; Wilczek, M. Nuclear magnetic dipole moments from NMR spectra. *Chem. Phys. Lett.* **2005**, *411*, 111–116. [CrossRef]
5. Jaszuński, M.; Antušek, A.; Garbacz, P.; Jackowski, K.; Makulski, W.; Wilczek, M. The determination of accurate nuclear magnetic dipole moments and direct measurement of NMR shielding constans. *Prog. Nucl. Magn. Reson. Spectrosc.* **2012**, *67*, 49–63. [CrossRef]
6. Zhao, E. Recent progress in theoretical studies of nuclear magnetic moments. *Chin. Sci. Bull.* **2012**, *57*, 4394–4399. [CrossRef]
7. Forman, P. Molecular beam measurements of nuclear moments before magnetic resonance. *Ann. Sci.* **1998**, *55*, 111–160. [CrossRef]
8. Jameson, C.J. The Noble Gases. In *Multinuclear NMR*; Mason, L., Ed.; Springer: Boston, MA, USA, 1987; Chapter 18; pp. 463–477. [CrossRef]
9. Jevremović, T. Nuclear Theory. In *Nuclear Principles in Engineering*; Springer: Boston, MA, USA, 2005; Chapter 3; pp. 61–126. [CrossRef]
10. Keeler, J. *Understanding NMR Spectroscopy*, 2nd ed.; John Wiley & Sons: Chichester, UK, 2010; ISBN 978-0-470-74609-7.
11. Mohr, P.J.; Newell, D.B.; Taylor, B.N. CODATA Recommended Values of the Fundamental Physical Constants: 2014. *Rev. Mod. Phys.* **2016**, *88*, 035009-1–035009-11. [CrossRef]
12. Jaszuński, M.; Jackowski, K. Nuclear Magnetic Dipole Moments from NMR Spectra—Quantum Chemistry and Experiment. In *Precision Physics of Simple Atoms and Molecules*; Karshenboim, S.G., Ed.; Lecture Notes in Physics; Springer: Berlin/Heidelberg, Germany, 2008; Volume 745, pp. 233–260. [CrossRef]
13. Dymond, J.D.; Marsh, K.N.; Wilhoit, R.C. *Virial Coefficients of Pure Gases and Mixtures*; Fenkel, M., Marsch, K.N., Eds.; Springer: Berlin/Heidelberg, Germany, 2003; ISBN 978-3-540-44340-7.
14. Jameson, C.J. Effects of Intermolecular Interactions and Intramolecular Dynamics on Nuclear Resonance. *Bull. Magn. Reson.* **1981**, *3*, 3–28.
15. Antušek, A.; Repisky, M. NMR absolute shielding scales and nuclear magnetic dipole moments of transition metal nuclei. *Phys. Chem. Chem. Phys.* **2020**, *22*, 7065–7076. [CrossRef]
16. Jameson, C.J. *Chemical Shift Scales on an Absolute Basis*; eMagRes; John Wiley & Sons: Hoboken, NJ, USA, 2011. [CrossRef]
17. Garbacz, P.; Jackowski, K.; Makulski, W.; Wasylishen, R.E. Nuclear Magnetic Shielding for Hydrogen in Selected Isolated Molecules. *J. Phys.Chem. A* **2012**, *116*, 11896–11904. [CrossRef]
18. Jackowski, K.; Makulski, W.; Szyprowska, A.; Antušek, A.; Jaszuński, M.; Jusélius, J. NMR shielding constants in BF_3 and magnetic dipole moments of ^{10}B and ^{11}B nuclei. *J. Chem. Phys.* **2009**, *130*, 044309-1–044309-5. [CrossRef]
19. Makulski, W.; Szyprowska, A.; Jackowski, K. Precise determination of the ^{13}C nuclear magnetic moment from ^{13}C, ^{3}He and ^{1}H NMR measurements in the gas phase. *Chem. Phys. Lett.* **2011**, *511*, 224–228. [CrossRef]
20. Nierenberg, W.A. Atomic beam magnetic resonance. *Physica* **1967**, *33*, 18–28. [CrossRef]
21. Penselin, S. Recent Developments and Results of the Atomic-Beam Magnetic-Resonance Method. In *Progress in Atomic Spectroscopy: Physics of Atoms and Molecules*; Hanle, W., Kleinpoppen, H., Eds.; Springer: Boston, MA, USA, 1978; pp. 463–490. [CrossRef]
22. Kellogg, J.M.B.; Rabi, I.I.; Ramsey, N.F., Jr.; Zacharias, J.R. The Magnetic Moments of the Proton and the Deuteron. The Radiofrequency Spectrum of H_2 in Various Magnetic Fields. *Phys. Rev.* **1939**, *56*, 728. [CrossRef]

23. Makulski, W. The radiofrequency NMR spectra of lithium salts in water; Reevaluation of Nuclear Magnetic Moments for ^{6}Li and ^{7}Li nuclei. *Magnetochemistry* **2018**, *4*, 9. [CrossRef]

24. Kaufman, S.L. High-resolution laser spectroscopy in fast beams. *Opt. Commun.* **1976**, *17*, 309–312. [CrossRef]

25. Geithner, W.; Georg, U.; Kappertz, S.; Keim, M.; Klein, A.; Lievens, P.; Neugart, R.; Neuroth, M.; Vermeeren, L.; Wilbert, S. Measurement of nuclear moments and radii by collinear laser spectroscopy and by β-NMR spectroscopy. *Hyperfine Interact.* **2000**, *129*, 271–288. [CrossRef]

26. Mihara, M. Fundamentals of β-NMR and its New Developments in Materials Science Studies. *Hyomen Kagaku* **2017**, *38*, 188–193. [CrossRef]

27. Abov, Y.G.; Gulko, A.D.; Dzheparov, F.S. Beta-NMR spectroscopy: Modern state and prospects. *Phys. At. Nucl.* **2006**, *69*, 1701–1710. [CrossRef]

28. Rubin, Y.; Wang, G.-W.; Jarrosson, T.; Bartberger, M.; Houk, K.N.; Schick, G.; Saunders, M.; Cross, R.J. Insertion of Helium and Molecular Hydrogen Through the Orifice of an Open Fullerene. *Angew. Chem. Int. Ed. Engl.* **2001**, *40*, 1543–1546. [CrossRef]

29. Baum, E.M.; Ernesti, M.C.; Knox, H.D.; Miller, T.R.; Watson, A.M. *Nuclides and Isotopes: Chart of the Nuclides*, 17th ed.; Knolls Atomic Power Lab, Bechtel: West Mifflin, PA, USA, 2010; Available online: https://www.nuclidechart.com/xcart/ (accessed on 20 November 2020).

30. Kouzes, R.T. *The ^{3}He Supply Problem*; Prepared for the U.S. Department of Energy; U.S. Department of Energy: Washington, DC, USA, 2009. [CrossRef]

31. Herzberg, G.; Douglas, A.E. The Nuclear Spin of He3. *Phys. Rev.* **1949**, *76*, 1529. [CrossRef]

32. Klein, M.P.; Holder, B.E. Determination of the Sign of the He^3 Nuclear Magnetic Moment. *Phys. Rev.* **1957**, *106*, 837–838. [CrossRef]

33. Anderson, H.L.; Novick, A. Magnetic moment of He^3. *Phys. Rev.* **1948**, *73*, 919. [CrossRef]

34. Anderson, H.L. Precise Measurement of the Gyromagnetic Ratio of He^3. *Phys. Rev.* **1949**, *76*, 1460–1470. [CrossRef]

35. Williams, W.L.; Hughes, V.W. Magnetic Moment and hfs Anomaly for He^3. *Phys. Rev.* **1969**, *185*, 1251–1255. [CrossRef]

36. Neronov, Y.I.; Barzakh, A.E. Determination of the magnetic moment of the He3 nucleus with an error of 2×10^{-6}%. *Zh. Eksp. Teor. Fiz.* **1978**, *75*, 1521–1540.

37. Belyi, V.A.; Il'ina, E.A.; Shifrin, V.Y. Experimental determination of the magnetic moments ratio for helium-3 and proton nuclei. *Meas. Tech.* **1986**, *29*, 613–616. [CrossRef]

38. Flowers, J.L.; Petley, B.W.; Richards, M.G. A measurement of the nuclear magnetic moment of the helium-3 atom in terms of that of the proton. *Metrologia* **1993**, *30*, 75–87. [CrossRef]

39. Hoffman, R.E.; Becker, E.D. Temperature dependence of the ^{1}H chemical shift of tetramethylsilane in chloroform, methanol, and dimethylsulfoxide. *J. Magn. Reson.* **2005**, *176*, 87–98. [CrossRef]

40. Jackowski, K.; Jaszuński, M.; Kamieński, B.; Wilczek, M. NMR frequency and magnetic dipole moment of ^{3}He nucleus. *J. Magn. Reson.* **2008**, *193*, 147–149. [CrossRef]

41. Neronov, Y.I.; Seregin, N.N. High-Precision Evaluation of the Magnetic Moment of the Helion. *J. Exp. Theor. Phys.* **2012**, *115*, 777–781. [CrossRef]

42. Aruev, N.N.; Neronov, Y.I. Gas Samples with a Mixture of Hydrogen Isotopes and ^{3}He for NMR Spectroscopy and Estimation of the Magnetic Moment of the ^{3}He Nucleus. *Zhurnal Tekhnicheskoi Fiz.* **2012**, *82*, 116–121. [CrossRef]

43. Rudziński, A.; Puchalski, M.; Pachucki, K. Relativistic QED and nuclear mass effects in the magnetic shielding of ^{3}He. *J. Chem. Phys.* **2009**, *130*, 244102. [CrossRef] [PubMed]

44. Schneider, G.; Mooser, A.; Bohman, M.; Schön, N.; Harrington, J.; Higuchi, T.; Nagahama, H.; Sellner, S.; Smorra, S.; Blaum, K.; et al. Double-trap measurement of the proton magnetic moment at 0.3 parts per billion precision. *Science* **2017**, *358*, 1081–1084. [CrossRef] [PubMed]

45. Stone, N.J. *Table of Nuclear Magnetic Dipole and Electric Quadrupole Moments*; IAEA Nuclear Data Section, Vienna International Centre: Vienna, Austria, 2014; Available online: http://www-nds.iaea.org/publications (accessed on 12 August 2019).

46. Jackowski, K.; Jaszuński, M.; Wilczek, M. Alternative Approach to the Standardization of NMR Spectra. Direct Measurement of Nuclear Magnetic Shielding in Molecules. *J. Phys. Chem. A* **2010**, *114*, 2471–2475. [CrossRef] [PubMed]

47. LaTourrette, J.T.; Quinn, W.E.; Ramsey, N.F. Magnetic moment of Ne^{21}. *Phys. Rev.* **1957**, *107*, 1202. [CrossRef]

48. Makulski, W.; Garbacz, P. Gas-phase ^{21}Ne NMR studies and the nuclear magnetic dipole moment of neon-21. *Magn. Reson. Chem.* **2020**, *58*, 648–652. [CrossRef]

49. Kozioł, K.; Aucar, A.; Aucar, G. Relativistic and QED effects on NMR magnetic shielding constant of neutral and ionized atoms and diatomic molecules. *J. Chem. Phys.* **2019**, *150*, 184301-1–184301-14. [CrossRef]

50. Chupp, T.E.; Oteiza, E.R.; Richardson, J.M.; White, T.R. Precision frequency measurements with polarized ³He, ²¹Ne, and ¹²⁹Xe atoms. *Phys. Rev. A* **1988**, *38*, 3998–4003. [CrossRef]

51. Sagawa, H.; Zhou, X.R.; Zhang, X.Z.; Suzuki, T. Deformations and electromagnetic moments in carbon and neon isotopes. *Phys. Rev. C* **2004**, *70*, 054316-1–054316-14. [CrossRef]

52. Geithner, W.; Brown, B.A.; Hilligsøe, K.M.; Kappertz, S.K.; Keim, M.; Kotrotsios, G.; Lievens, P.; Marinova, K.; Neugart, R.; Simon, H.; et al. Nuclear moments of neon isotopes in the range from ¹⁷Ne at the proton drip line to neutron-rich ²⁵Ne. *Phys. Rev. C* **2005**, *71*, 064319-1–064319-7. [CrossRef]

53. Marinova, K.; Geithner, W.; Kowalska, M.; Blaum, K.; Kappertz, S.; Keim, M.; Kloos, S.; Kotrotsios, G.; Lievens, P.; Neugart, R.; et al. Charge radii of neon isotopes across the *sd* neutron shell. *Phys. Rev. C* **2011**, *84*, 034313-1–034313-12. [CrossRef]

54. Jiang, W.; Williams, W.D.; Bailey, K.; Davis, A.M.; Hu, S.-M.; Lu, Z.-T.; O'Connor, T.P.; Purtschert, R.; Sturchio, N.C.; Su, Y.R.; et al. Ar-39 Detection at the 10-16 Isotopic Abundance Level with Atom Trap Trace Analysis. *Phys. Rev. Lett.* **2011**, *106*, 103001. [CrossRef] [PubMed]

55. Klein, A.; Brown, B.A.; Georg, U.; Keim, M.; Lievens, P.; Neugart, R.; Neuroth, M.; Silverans, R.E.; Vermeeren, L. Moments and mean square charge radii of short-lived argon isotopes. *Nucl. Phys.* **1996**, *607*, 1–22. [CrossRef]

56. Hoffman, R. Multinuclear NMR Website, Institute of Chemistry, The Hebrew University of Jerusalem, Jerusalem, Israel. Available online: http://chem.ch.huji.ac.il/nmr/techniques/1d/multi.html (accessed on 20 November 2020).

57. Jameson, C.J.; de Dios, A.C. The nuclear magnetic shielding as a function of intermolecular separation. *J. Chem. Phys.* **1993**, *98*, 2208–2217. [CrossRef]

58. Blaum, K.; Geithner, W.; Lassen, J.; Lievens, P.; Marinova, K.; Neugart, R. Nuclear moments and charge radii of argon isotopes between the neutron-shell closures N = 20 and N = 28. *Nucl. Phys. A* **2008**, *799*, 30–45. [CrossRef]

59. Heim, M.; Fritsch, A.; Schuh, A.; Shore, A.; Thoennessen, M. Discovery of the Krypton Isotopes. *At. Data Nucl. Data Tables* **2010**, *96*, 333–340. [CrossRef]

60. Lehmann, J.F.; Marcier, H.P.A.; Schrobilgen, G.J. The chemistry of krypton. *Coord. Chem. Rev.* **2002**, *233–234*, 1–39. [CrossRef]

61. Kellog, J.B.M.; Millman, S. The Molecular Beam Magnetic Resonance Method. The Radiofrequency Spectra of Atoms and Molecules. *Rev. Mod. Phys.* **1946**, *18*, 323. [CrossRef]

62. Brinkman, D. The nuclear magnetic moments of ⁸³Kr and ³⁹K. *Phys. Lett.* **1968**, *27A*, 466–467. [CrossRef]

63. Brinkmann, D. Verschiebung des lokalen magnetischen Feldes in der Kernresonanz von Edelgasen. *Helv. Phys. Acta* **1968**, *41*, 367–384. [CrossRef]

64. Makulski, W. ⁸³Kr nuclear magnetic moment in terms of that of ³He. *Magn. Reson. Chem.* **2014**, *52*, 430–434. [CrossRef] [PubMed]

65. Keim, M.; Arnold, E.; Borchers, W.; Georg, U.; Klein, A.; Neugart, R.; Vermeeren, L.; Silverans, R.E. Lievens, Laser-spectroscopy measurements of ⁷²⁻⁹⁶Kr spins, moments and charge radii. *Nucl. Phys.* **1995**, *A586*, 219–239. [CrossRef]

66. Huston, J.L. Chemical and Physical Properties of Some Xenon Compounds. *Inorg. Chem.* **1982**, *21*, 685–688. [CrossRef]

67. Raftery, D. Xenon NMR spectroscopy. *Ann. Rep. NMR Spectrosc.* **2006**, *57*, 205–270.

68. Kopfermann, H.; Rindal, E. Über die Kernmomente des Xenons. *Zeitschrift für Physik* **1934**, *87*, 460–469. [CrossRef]

69. Butscher, R.; Wäckerle, G.; Mehring, M. Nuclear quadrupole interaction of highly polarized gas phase ¹³¹Xe with a glass surface. *J. Chem. Phys.* **1994**, *100*, 6923–6933. [CrossRef]

70. Meersmann, T.; Haake, M. Magnetic Field Dependent Xenon-131 Quadrupolar Splitting in Gas and Liquid Phase NMR. *Phys. Rev. Lett.* **1998**, *81*, 1211–1214. [CrossRef]

71. Proctor, W.G.; Yu, F.C. On the Nuclear Magnetic Moments of Several Stable Isotopes. *Phys. Rev.* **1951**, *81*, 20–30. [CrossRef]

72. Brun, E.; Oeser, J.; Staub, H.H.; Telschow, C.G. The Nuclear Magnetic Moments of Xe¹²⁹ and Xe¹³¹. *Phys. Rev.* **1954**, *93*, 904. [CrossRef]

73. Brinkmann, D. Die magnetischen Momente von Xe^{129} und Xe^{131}. *Helv. Phys. Acta* **1963**, *36*, 413–414. [CrossRef]

74. Pfeffer, M.; Lutz, O. ^{129}Xe Gas NMR-Spectroscopy and Imaging with a Whole-Body Imager. *J. Magn. Reson.* **1994**, *108*, 106–109. [CrossRef]

75. Makulski, W. ^{129}Xe and ^{131}Xe Nuclear Magnetic Dipole Moments from Gas Phase NMR Spectra. *Magn. Reson. Chem.* **2015**, *53*, 273–279. [CrossRef] [PubMed]

76. Fan, I.; Knappe-Grüneberg, S.; Voigt, J.; Kilian, W.; Burgho, M.; Stollfuss, D.; Schnabel, A.; Wübbeler, G.; Bodner, O.; Elster, C.; et al. Direct measurement of the γHe/γXe ratio at ultralow magnetic field. *J. Phys. Conf. Ser.* **2016**, *723*, 012045. [CrossRef]

77. Kitano, M.; Calaprice, F.P.; Pitt, M.L.; Clayhold, J.; Happer, W.; Kadar-Kallen, M.; Musolf, M.; Ulm, G.; Wendt, K.; Chupp, T.; et al. Nuclear Orientation of Radon Isotopes by Spin Exchange Optical Pumping. *Phys. Rev. Lett.* **1988**, *60*, 2133–2136. [CrossRef]

78. Karol, P.J.; Barber, R.C.; Sherrill, B.M.; Vardaci, E.; Yamazaki, T. Discovery of the element with atomic number $Z = 118$ completing the 7th row of the periodic table (IUPAC Technical Report). *Pure Appl. Chem.* **2015**, *88*, 155–160. [CrossRef]

79. Jackson Kimball, D.F. Nuclear spin content and constraints on exotic spin-dependent couplings. *New J. Phys.* **2015**, *17*, 073008. [CrossRef]

80. Pirahmadian, M.H.; Ghahramany, N. Helium-3 magnetic dipole moment determination by using quark constituents for all possible baryon formations. *Results Phys.* **2017**, *7*, 2771–2774. [CrossRef]

81. Vanasse, J. Charge and magnetic properties of three-nucleon systems in pionless effective field theory. *Phys. Rev. C* **2017**, *98*, 034003. [CrossRef]

82. Saxena, A.; Srivastava, P.C. First-principles results for electromagnetic properties of *sd* shell nuclei. *Phys. Rev. C* **2017**, *96*, 024316. [CrossRef]

83. Gustavsson, M.G.H.; Mårtensson-Pendrill, A.-M. Need for remeasurements of nuclear magnetic dipole moments. *Phys. Rev. A* **1998**, *58*, 3611–3618. [CrossRef]

84. Lide, D.R. (Ed.) *CRC Handbook of Chemistry and Physics*; CRC Press: Boca Raton, FL, USA, 2006; Volume 81, ISBN1 978-0849304811. ISBN2 0849304814.

85. Vaara, J.; Pyykko, P. Relativistic, nearly basis-set-limit nuclear magnetic shielding constants of the rare gases He–Rn: A way to absolute nuclear magnetic resonance shielding scales. *J. Chem. Phys.* **2003**, *118*, 2973–2976. [CrossRef]

86. Komorovský, S.; Repiský, M.; Malkina, O.L.; Malkin, V.G. Fully relativistic calculations of NMR shielding tensors using restricted magnetically balanced basis and gauge including atomic orbitals. *J. Chem. Phys.* **2010**, *132*, 154101. [CrossRef] [PubMed]

87. Watkins, T. *The Profile of Magnetic Dipole Moments of the Nuclides of the Same Proton Number as a Function of Their Neutron Number*; Silicon Valley and Tornado Alley; San Jose State University: San Jose, CA, USA; Available online: applet-magic.com (accessed on 20 November 2020).

88. Mooser, A.; Rischka, A.; Schneider, A.; Blaum, K.; Ulmer, S.; Walz, J. A New Experiment for the Measurement of the g-Factors of ^{3}He$^+$ and ^{3}He^{2+}. *J. Phys. Conf. Ser.* **2018**, *1138*, 012004. [CrossRef]

89. Lilburn, D.M.L.; Pavlovskaya, G.E.; Meersmann, T. Perspectives of hyperpolarized noble gas MRI beyond ^{3}He. *J. Magn. Reson.* **2013**, *229*, 173–186. [CrossRef]

90. Berthault, P.; Huber, G.; Desvaux, H. Biosensing using laser-polarized xenon NMR/MRI. *Prog. Nucl. Magn. Reson.Spectrosc.* **2009**, *55*, 35–60. [CrossRef]

91. Kupka, T.; Stachów, M.; Stobiński, L.; Kaminský, J. ^{3}He NMR: From free gas to its encapsulation in fullerene. *Magn. Reson. Chem.* **2013**, *51*, 463–468. [CrossRef]

Publisher's Note: MDPI stays neutral with regard to jurisdictional claims in published maps and institutional affiliations.